HOSTED BY

ELSEVIER

Available online at www.sciencedirect.com

ScienceDirect

Soils and Foundations 63 (2023) 101322

www.elsevier.com/locate/sandf

Technical Paper

Analysis of the behaviour of retaining structures through a novel data interpretation approach

A. Dobrisan [a,*], S.K. Haigh [a], C. Deng [a], Y. Ishihara [b]

[a] *Schofield Centre, Department of Engineering, University of Cambridge, Cambridge, UK*
[b] *Scientific Research Section, Giken Ltd., Kochi, Japan*

Received 9 November 2022; received in revised form 5 April 2023; accepted 18 April 2023
Available online 12 May 2023

Abstract

Retaining structures are generally designed to satisfy serviceability limits on allowed deflections while also providing sufficient strength to carry the bending moment caused by the soil pressure acting on the wall in tandem with any applied loads. Since wall displacement and mobilised soil pressure are the most important design parameters, direct measurement would be ideal, however instrumentation limitations leave the measurement of wall curvature using strain gauges and rotation using inclinometers as the industry standard for retaining wall monitoring. Pressure and deflection are normally inferred from these discrete, sparse and potentially inaccurate measurements through beam theory by fitting the discrete data to obtain differentiable continuous curves. Conventional fitting methods cannot simultaneously fit data from different types of instrumentation like inclinometers and strain gauges and there is generally little flexibility in addressing issues when the fits do not make geotechnical sense. A novel fitting approach is developed to address these shortcomings, with the ability to pull together imperfect data from a multitude of instruments (strain gauges, inclinometers, displacement transducers etc.) into a cohesive prediction. The method is validated based on field and centrifuge data in which it outperforms existing fitting solutions. This novel approach significantly simplifies data analysis by enabling practising engineers and researchers to simply input all instrument data from a retaining structure and retrieve sensible and accurate predictions of the parameters of soil-structure interaction which are compatible with all data measured and insensitive to measurement errors to a high degree.

Keywords: Data fitting; Retaining walls; Lateral loading of piles; Discrete measurements; Multifit

1. Introduction

Reliably analysing and interpreting data from experiments and field studies is a critical aspect in advancing our understanding of geotechnical behaviour leading to better and more robust design methods. Some of the most researched structures are retaining walls due to their ubiquitous use in geotechnical projects. Retaining wall designs are generally developed to satisfy design limits on wall deflections y, while providing wall strength sufficient to carry the bending moment distribution M caused by the soil pressure acting on the wall p together with any applied loads.

Since wall displacement and soil pressure are the most important properties in characterising the soil-structure interaction, it would be attractive to measure these directly. Unfortunately, while measurement of wall displacements above the excavation level is possible if a suitable stable reference position is available, direct measurement of displacements beneath the ground is currently extremely difficult. While earth pressures can be measured using pressure cells, the values measured can be highly inaccurate

* Corresponding author.
E-mail addresses: andrei@dobrisan.uk (A. Dobrisan), skh20@cam.ac.uk (S.K. Haigh), cd567@cantab.ac.uk (C. Deng), ishihara@giken.com (Y. Ishihara).

https://doi.org/10.1016/j.sandf.2023.101322

Nomenclature

Notation

p	Net Soil Pressure
S	Shear Force
M	Bending Moment
κ	Curvature
θ	Rotation
y	Wall displacement or Pile Deflection
z	Depth from ground level
B	Bending Stiffness also known as Flexural Rigidity
K_a	Active lateral earth pressure coefficient
K_p	Passive lateral earth pressure coefficient
PIV	Particle Image Velocimetry
LVDT	Linear Variable Displacement Transducer
ULS	Ultimate Limit State

(Weiler and Kulhawy, 1982) owing to distortions of the gauge diaphragms changing the earth pressures acting upon them. New technologies such as null-gauges (Talesnick, 2005) can substantially increase the accuracy of these measurements by applying a balancing pressure inside the instrument to achieve zero gauge deformation. While these instruments have been used to measure earth pressures in geotechnical research (Burali d'Arezzo et al., 2015) these high accuracy complex instruments are not generally used in practice. These limitations in measuring the key parameters for design leave the measurement of wall curvature κ using strain gauges and wall inclination θ using inclinometers as the industry standard for monitoring of retaining wall distortion with wall translations and rotations at the surface being used to give integration boundary conditions to infer rigid body movement. These measurements can then be used to deduce other deformation parameters through Euler–Bernoulli beam theory (Timoshenko, 1953) which links all the salient properties of a retaining wall together:

$$p = \frac{\mathrm{d}S}{\mathrm{d}z} = \frac{\mathrm{d}^2M}{\mathrm{d}z^2} = -B\frac{\mathrm{d}^2\kappa}{\mathrm{d}z^2} = -B\frac{\mathrm{d}^3\theta}{\mathrm{d}z^3} = -B\frac{\mathrm{d}^4y}{\mathrm{d}z^4} \tag{1}$$

where B is bending stiffness and z is a coordinate variable along the depth of the wall. p is the *net soil pressure*, equal to the difference between the active and passive earth pressures acting on the wall. Employing Euler–Bernoulli assumes the wall analysis is carried out in the linear elastic regime, i.e. $B(z) = constant$. Non-linearities e.g. stress–strain relationship in reinforced concrete walls past the first "cracking" moment can be modelled with a variable $B(z)$, but for simplicity this paper will only concern itself with case studies of retaining structures in the elastic regime of loading.

If the continuous distribution of any one parameter in the Euler chain in Eq. (1) is known and appropriate boundary conditions are given it can be used to calculate all other wall properties. Experimental readings of curvature (moment) or rotation are, however, normally discrete, sparse and potentially inaccurate. A continuous profile of κ or θ hence needs to be extrapolated from the discrete data set to be differentiated down to p and integrated up to y. A common use for these derived profiles of p and y is in plotting $p-y$ curves at various depths in order to interpret the mobilisation of active and passive earth pressure with wall movement in a manner which can lead to performance-based design procedures (Deng et al., 2021).

In order to make an effective design procedure it is paramount that the derived values for p and y are as accurate as possible. This requires high quality continuous fits for the discrete data of curvature or rotation. In most cases, researchers analysing such retaining wall data choose to employ one of two techniques. Either they use a single high order polynomial to fit the data such that the root-mean-square (RMS) error between the fit and the data is minimised, or they employ splines, piecewise lower order polynomials that strictly pass through all data points. However, both techniques present significant shortcomings. As shown by Haiderali and Madabhushi (2016), fitting data from embedded structures using a single polynomial is very sensitive to the polynomial order chosen. Moreover, the fit polynomial may exhibit large unwanted oscillations when its order approaches the number of measurement points along the retaining wall. Conversely, fitting using a lower order polynomial presents its own challenges: the differentiation chain in Eq. (1) implies the earth pressure distribution will be fitted by a polynomial two orders lower than that for bending moment and three orders lower than that for rotation. Therefore using a low order polynomial to fit either moment or rotation data will significantly limit the earth pressure distributions that can be predicted. This issue is amplified in the case of spline fitting as splines are typically assembled from cubic polynomials, giving linear predictions of earth pressure distribution between measurement points when fitted to bending moments and constant values when fitted to inclinations. Furthermore, because splines are designed to pass through all data points, they exhibit high sensitivity to noise in the experimental measurements.

A different approach to the problem of fitting discrete data is to apply Bayesian statistics on either polynomial or spline functions and obtain a range of probable values for the coefficients of these functions. This statistical view on fitting, whilst not frequently employed in geotechnical

problems, enhances the traditional techniques described in the previous paragraph by quantifying the spread of possible fits. However, retaining wall data on moment or wall rotation is frequently sparse, i.e. only available at a small number of locations on the wall, which means the results of Bayesian regression will be skewed by the selected priors. The priors represent the researcher's initial guess of what the distribution of polynomial or spline coefficients should look like. As shown by Diaconis and Freedman (1986) improper priors can result in inconsistent Bayes estimates, i.e. the Bayes results will not converge around the correct fit for the moment or inclination data.

A significant issue with both spline and high-order polynomial fitting, whether using a traditional or Bayesian approach, is that if experimental data is available from multiple instrument types, e.g. strain gauges and inclinometers, there is no straightforward way to merge these data sets into a single fit. Instead, the researcher is in the non-ideal situation of needing to pick one instrument type to "trust" since it is unlikely that integration of the M profile obtained by fitting the strain gauge data will agree precisely with the inclinometer data and vice versa. Moreover, the derived p and y profiles may sometimes conflict with expected behaviour, either directly in predicting earth pressures which violate plausible values or when predicted earth-pressures and displacements are not compatible. There is generally very little option to use the observed discrepancy as feedback to improve the fits.

1.1. Embedded cantilever retaining walls in sand (Li and Lehane, 2010)

To illustrate the issues presented, the results from a well-instrumented, full-scale cantilevered retaining wall in sand presented by Li and Lehane (2010) are considered. In-situ test data recorded within 20 m from the wall is shown in Fig. 1. A shallow pressure bulb about 0.5 m deep can be inferred from both the horizontal stress and the CPT strength plots.

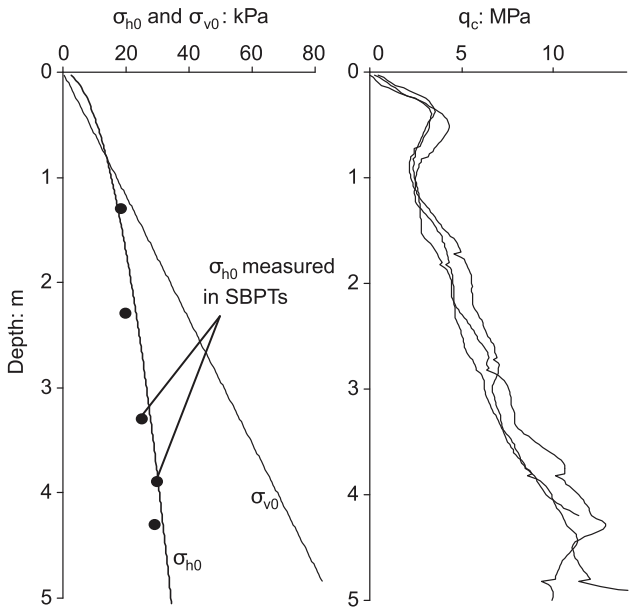

Fig. 1. In situ test data from Li and Lehane (2010).

The 3.7 m deep wall was created using four piles instrumented with strain gauges at 1.3 m, 2.3 m, 2.7 m, 3.1 m from the top of the wall and adjustments were made to remove thermal effects from the bending moment data. Wall rotation readings were made using a 500mm inclinometer torpedo at 0.25 m intervals with readings at the same depth being averaged to diminish operator errors. The displacement at the top of the retaining wall was monitored optically through mounted targets with calibration procedures and Particle Image Velocimetry (PIV) being used to achieve high quality accurate data.

Fig. 2a shows the measured bending moment data and the spline fitted to it at the instance when excavation reached 2.2 m depth. In an attempt to increase reliability the researchers took extra care to impose physical constraints on the fit to ensure that:

- there was zero moment, shear and pressure at wall top ($z = 0$);
- there was zero moment at the wall base;
- shear at the wall base was less than a maximum shear limit derived from the pile's full weight;
- a local maximum for shear existed at the excavation level owing to the reversal of loading direction.

The final assumption can be considered an approximate one since the reversal of loading direction would be expected to occur a small distance below the excavation depth, at the point where the passive earth pressure matches the active one.

The rotation data from inclinometers was integrated to calculate the wall deflection with the PIV top measurement used as the integration constant (Fig. 2c).

For the most part, the data agree well with geotechnical experience. At shallow depths below the top of the retaining wall the net pressure profile (Fig. 2b) shows negative values consistent with an active soil region. Around the excavation depth of 2.2 m the net pressure abruptly changes to positive values consistent with passive earth pressures developing on the excavated side and resisting the retaining wall's movement.

From the net pressure profile we can also observe a second change in sign at around 3.3 m depth which would suggest that passive earth pressures are being generated on the retained side. This might indicate the presence of a rotation point around 3.3 m depth; a rotation point is also the most likely explanation for the predicted negative value of shear force at the base of the retaining wall, i.e. the force is pointing towards the excavated side (see Fig. 2a). However, this is contradicted by the wall deflection profile in Fig. 2c which shows an overall translation towards the excavated side with the expectation of positive base shear, i.e. pointing back towards the retained side. Hence the deflections

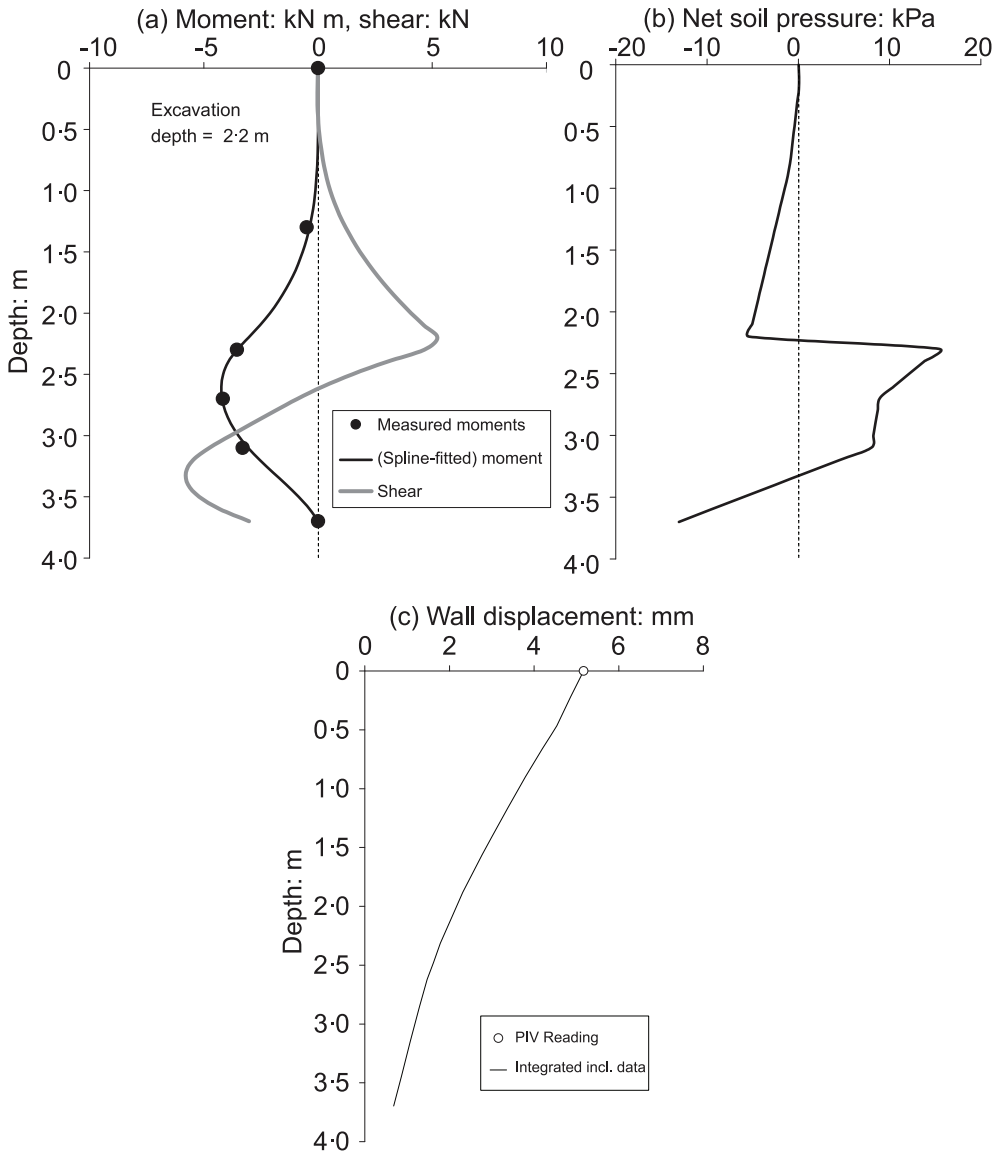

Fig. 2. Moment, shear, net pressures and lateral wall displacement derived for excavation depth 2.2 m from Li and Lehane (2010).

inferred from inclination and PIV data are inconsistent with the shear profile derived from the strain gauge data.

Using present techniques there is little that can be done to improve the fit and resolve this incompatibility. Even though deflection, shear and net pressure are part of the same derivation chain as shown by Eq. (1) there is no straightforward way to pull together the measured data from PIV, inclinometers and strain gauges and analyse the wall in a unitary fashion. This paper introduces a new fitting routine, *multifit*, to aid in deriving and analysing retaining wall properties in a manner that addresses the shortcoming highlighted above.

2. Proposed fitting method

In designing a more robust fitting routine for geotechnical structures we first distilled down the high level problems identified above into equivalent mathematical conditions that the fit had to fulfil. It became apparent that a careful reconsideration of basic principles of fitting can lead to significant improvements. Firstly the issue of not being able to fit data from multiple instruments with a single fit can be addressed by making a small conceptual change to high order polynomial fitting. Generally, for a user-specified polynomial order, the polynomial coefficients are treated as variables and coefficients are found that minimise the RMS difference between the measured experimental value and the polynomial's prediction at the instrument location on the wall. If these readings represent the wall's rotation from inclinometer data then by simply differentiating the polynomial we can also evaluate the difference between the value that the polynomial's derivative takes at the location of the strain gauges and the strain gauge data. We can then calculate a total error term across all differentiation

levels to find a fit polynomial that minimises the total error with respect to all data. Because errors need to be amalgamated into a single term, we need to account for the different units of retaining wall properties, e.g. displacements being in mm and soil pressure in kPa.

Using the mean squared error to select the best-fit polynomial while informative, does not in any way give a representation of other possible polynomials that could fit the data almost as well but which might have substantially different shapes between measurement points. A theorem in mathematics, the Weierstrass approximation theorem (Weierstrass, 1885) states that any continuous function can be approximated by polynomials within any given error margin. Thus if we choose to fit data using polynomials with a high enough order, there will always exist polynomials that fit the retaining wall data, the true deflection and pressure profiles to a very high degree of accuracy since these profiles are continuous. The high quality Weierstrass polynomials may not however match the polynomial found through the standard RMS method. Even so, the presence of improved fits as predicted by the Weierstrass approximation theorem is encouraging. The authors suggest that a viable method to fit is to find the domain of all possible polynomials of a given high order that fit the data within specified error ranges rather than merely a singular polynomial. This domain is well understood mathematically as it features in significant problems such as linear programming (Dantzig, 1951). We can extract the possible solutions from the domain and select a central prediction together with confidence bounds for the obtained moment, deflection, pressure etc. With modern computational power this can be achieved with a reasonable run time on standard computers.

Short for multiple fitting, *multifit* implements the above ideas. It does not return a single fit to the discrete data, rather a family of polynomials of a given order that are a representative sample of all possible solutions to the problem of fitting the given data set within specified error bands. The user is then free to apply the statistics of their choice to obtain confidence bands for the values of net soil pressure, wall deflection etc. The procedure is outlined in the diagram shown in Fig. 3. Intuitively, the more information there is about the studied retaining wall, the less uncertainty there will be. *Multifit*'s output will then converge to the true deformation and soil pressure profiles. To this end, *multifit* was designed to accept detailed, diverse information about the retaining wall and importantly will not output any curve that does not satisfy **all input conditions**.

Data such as displacement measurements from lvdts, wall rotation from inclinometers and curvature readings from strain gauges can be used and evaluated simultaneously, offering a discernible advantage over standard fitting methods. In order to determine which fit functions are valid, *multifit* requires an estimate of the error associated with each experimental measurement. Since instrument error might have different sources, the program allows two types of error to be specified for each instrument. An

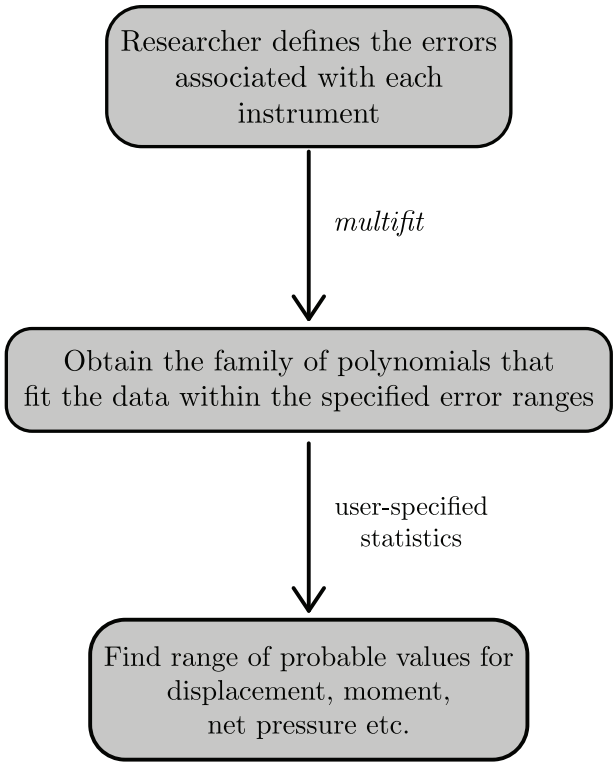

Fig. 3. Diagram of *multifit* procedure.

absolute error which could be the instrument's resolution (e.g. the minimum angle that can be read from an inclinometer) or an instrument's drift and a relative term which accounts for issues such as calibration errors. Setting both absolute and relative errors to zero signifies for *multifit* that the investigated property is known exactly at that point, for example zero moment existing at a retaining wall's free end.

Since *multifit* returns a large set of polynomials that satisfy the input requirements, finding the value of a property such as bending moment requires evaluation of the moment value from each polynomial in the set. This results in a range of possible moments that can be acting on the retaining wall at the considered depth. By applying statistics on the distribution of possible moment values, we can narrow down the result to a smaller range of probable moments. The analysis carried out in this paper takes the region of probable values as defined between the 20^{th} percentile and 80^{th} percentile such that 60% of the possible moment values lie within the band. The same approach can be used for all retaining wall properties. It is important to note that any type of statistics may be carried out on the output from *multifit*.

3. Experimental validation

3.1. Field data Li and Lehane (2010)

In order to test the analysis process detailed above against a high quality dataset for which problems have

been observed in using conventional fitting procedures, the data of Li and Lehane (2010) was reanalysed. *Multifit* allows us to derive fits consistent with the measured rotations, wall head displacement and bending moment data. As the measured inclination readings were not directly reported by Li and Lehane (2010), these were back-calculated from the displacement data in Fig. 2c. Fig. 4 shows the resulting wall inclinations on which scatter may be observed, likely due to the very small angles being measured.

To run the *multifit* analysis, error bands had to be assigned to each of the measurements. Per Li and Lehane (2010) the strain gauge data had 10% relative error so this error value was used and no absolute error term was assigned to the strain gauges. Li and Lehane (2010) does not list the error for the inclinometer data so an estimate was required. A conservative absolute error term of 0.015° was considered to allow for the jagged profile. A further 5% relative error term was used to widen the error bands and indicate the significant uncertainty in the errors of the inclination data. These bands are plotted in Fig. 6. For the displacement of the wall top which Li and Lehane (2010) obtained from an accurate PIV procedure a small 3% relative error was considered.

Generally, the resulting fits would be expected to be sensitive to the values of the user-defined errors, however use of *multifit* on typical retaining wall datasets has shown the effect to be minor when sensible error ranges are selected. Moreover, a significant underestimation of an instrument's true error range introduces an unwanted trade-off: the accuracy of the overall prediction is reduced for increased precision in fitting each individual measurement point. This leads to spurious oscillations between measurements for

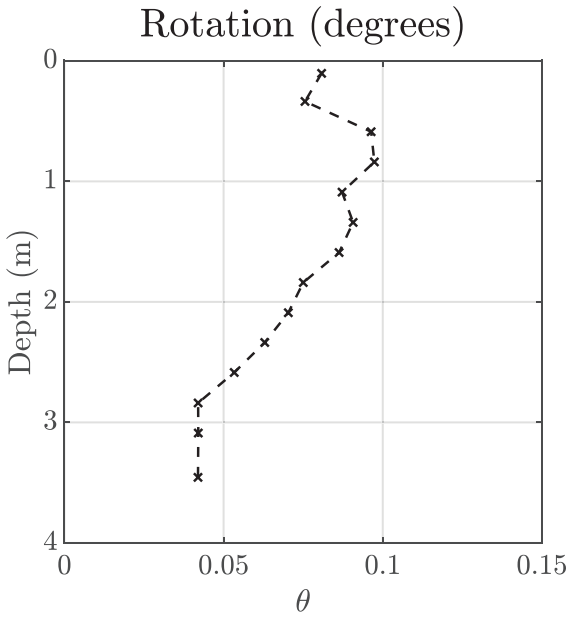

Fig. 4. Inclination data extrapolated from Fig. 2c from Li and Lehane (2010).

polynomial fitting. Since *multifit* aggregates results from the family of polynomials that fit the data set within the specified error bands, the *multifit* output will either also include oscillatory behaviour or, more likely, present an alternating profile with narrow confidence bands at measurement points and wide bands in between these to represent the uncertainty introduced by the unwanted oscillations of the individual polynomials in the set. Since this type of output is likely inconsistent with the expected behaviour as dictated by fundamental soil mechanics it makes it easy to spot and correct improper input.

As shown in the diagram in Fig. 3, once the errors are assigned, the *multifit* analysis can be run. In this case a 12^{th} order analysis was carried out. Twelve is the order of the polynomials fitting the parameter highest in the differentiation chain in Eq. (1) which is wall displacement in this particular example. Hence *multifit* returns the set of 12^{th} order polynomials which represent the possible wall displacement profiles so that the top displacement is within 3% of the PIV reading. Since the polynomial set is quite large, the band between the 20^{th} and 80^{th} percentiles is considered as described in the previous section.

A comparison between *multifit* predictions using 12^{th} order polynomials and the spline fits used by Li and Lehane (2010) is shown in Fig. 5. Both analysis procedures are consistent with the experimental measurements, that is to say the displacement, rotation (Fig. 6) and moment predictions are similar. Moreover, both fitting methods show a transition from active to passive earth pressure around the excavation depth of 2.2 m depth (Fig. 5b), in line with the expectation of significant passive resistance developing on the excavated side. The two fitting methods diverge however in their shear and net soil pressure predictions. As shown in Fig. 5a, *multifit* predicts a positive shear force at the base of the wall, i.e. pointing towards the retained side, which intuitively matches the fact that the wall as a whole moves into the excavated side (Fig. 5d). This resolves the inconsistency in the spline fit caused by the predicted negative base shear, inconsistency that was highlighted in Section 1.1. To achieve both the expected shear force behaviour as well as overall moment equilibrium, *multifit* predicts significant mobilisation of pressure on the retained side close to the toe of the wall (Fig. 5b).

Another difference between splines and *multifit* can be observed in the net pressure prediction at shallow depths (inset of Fig. 5b). Within the first 0.5 m of soil the spline fit predicts a very slow increase in pressure, whereas *multifit* identifies a pressure distribution which better correlates with the in situ strength data shown in Fig. 1.

A further distinction between the fit methods can be found in the rate of change of net soil pressure from active to passive at the excavation depth. The spline fit's abrupt change amounts to a K_p prediction of 14 ± 2 according to Li and Lehane (2010). This value seems large, given that Li and Lehane (2010) suggest a critical state friction angle of 33° for the site which equates to a limiting K_p of 3.4 and

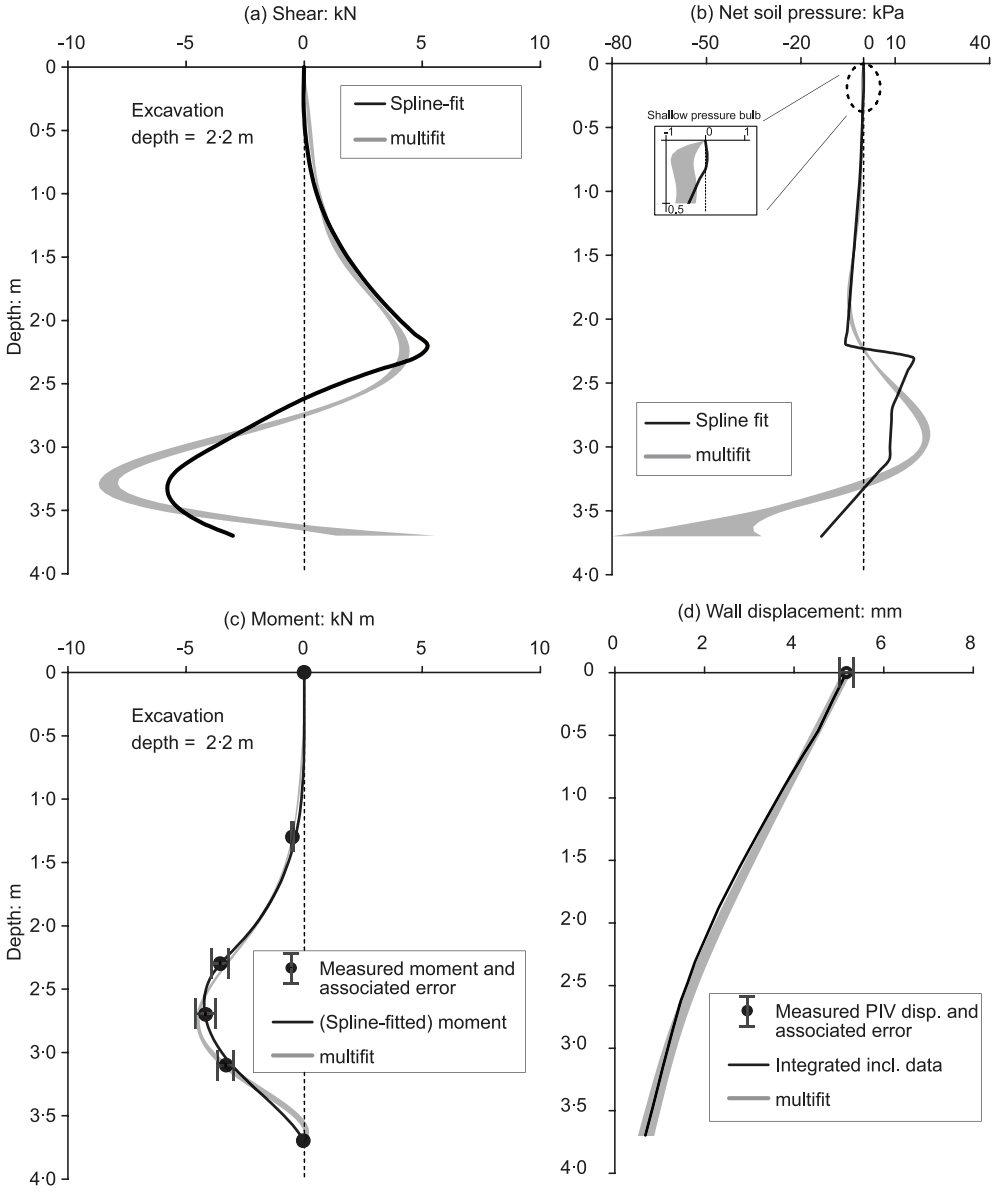

Fig. 5. Comparison between *multifit* and spline fitting.

K_a of 0.3 according to Coulomb theory. *Multifit's* transition from active to passive earth pressure amounts to a K prediction of about 2.0, which is closer to the theoretical limit. Even though this value seems sensible, it is important to note that *multifit* might under predict K if the order of the polynomials used to fit the data is too low, i.e. the curves are too smooth to properly capture the sudden change from active to passive pressures just below the excavation depth. This might be mitigated by increasing the order of the polynomials *multifit* uses to search for viable fits, however the trade-off to incrementing the polynomial order is an exponentially increasing computation time.

Overall, except for the potential under prediction in pressure gradient highlighted above, the *multifit* approach proved advantageous compared with traditional spline fitting by producing displacement, rotation, moment, shear and pressure curves which formed a consistent picture of the retaining wall properties that made geotechnical sense. This reflects the new perspectives that may be gained from existing data sets through this new approach.

3.2. Centrifuge data (Deng, 2020)

Centrifuge experiments are an invaluable tool in investigating the behaviour of geotechnical structures such as retaining walls. By subjecting a model scale setup to high g acceleration fields the stress–strain behaviour of a prototype structure can be replicated at model scale in the centrifuge. However, the large accelerations in these experiments may also affect the measurement devices, such as camera lenses distorting under g when conducting PIV image capture (White et al., 2003).

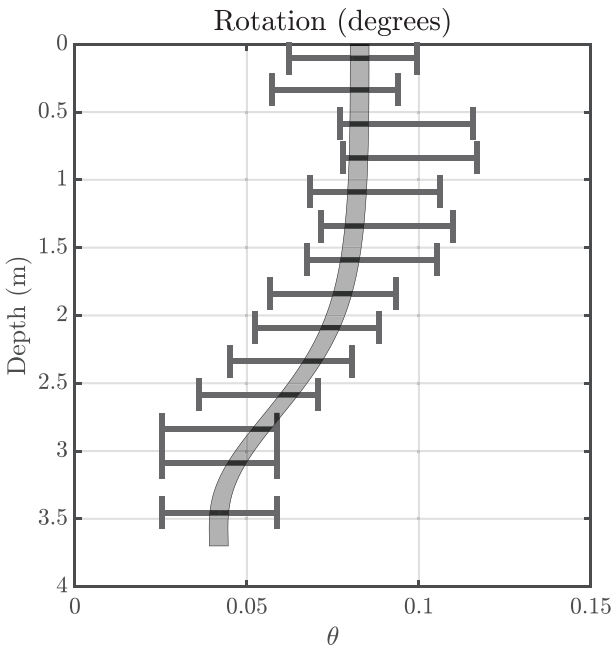

Fig. 6. Inclinometer data with error bars and *multifit* result.

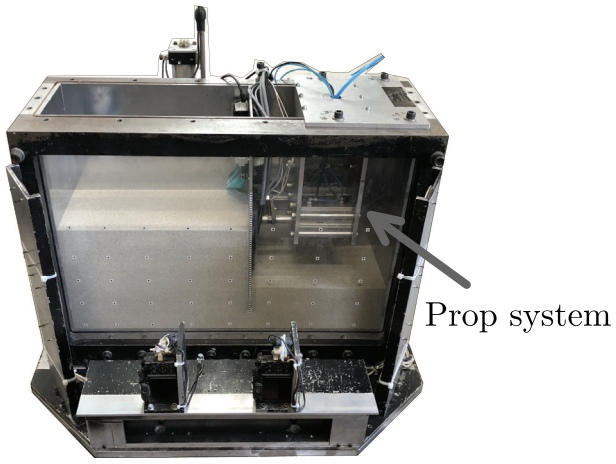

Fig. 7. General setup of the centrifuge experiment.

To validate whether *multifit* can be used to analyse data from centrifuge experiments the recorded behaviour of a retaining wall from a centrifuge test presented by Deng (2020) is investigated. The test setup, shown in Fig. 7, features a propped retaining wall, 250mm long, supporting a 168mm excavation at model scale. The package was swung up to 40g so the prototype investigated scales up by the same amount, i.e. the prototype wall is 10 m long and the excavation 6.72 m deep.

The wall was monitored through 15 full-bridge bending moment gauges placed at 0.8 m, 2.0 m, 3.2 m, 4.4 m, 5.6 m, 6.0 m, 6.4 m, 6.8 m, 7.2 m, 7.6 m, 8.0 m, 8.4 m, 8.8 m, 9.2 m, 9.6 m from the ground surface. The prop force was measured by load cells and PIV was used to capture wall deformation though the use of markers stuck to the side of the wall calibrated using further stationary markers on the perspex window as described by White et al. (2003). The retaining wall was also instrumented with Tekscan pressure sensing mats on both the retained and excavated sides to measure the mobilised soil pressure (Paikowsky and Hajduk, 1997).

Monitoring of deflection, bending moment, prop force and soil pressures simultaneously would seem to give a complete picture of the soil-structure interaction for this experiment, however, due to instrument errors, fits that satisfy the whole of the data set could not be found through standard methods. By selecting error bounds that allowed for instrumentation limitations, the *multifit* approach yielded encouraging results as shown in Fig. 8. It can be observed in Fig. 8 (plotted at prototype scale) that the error bounds are significantly larger than those considered for the field data from Li and Lehane (2010), mainly due to the need to account for centrifuge effects. As discussed in Section 2, instrument error may be thought of as being comprised of an absolute term linked to resolution or drift and a relative term which encompasses issues such as calibration errors. An instrument's relative error is the same between model and prototype, however the absolute error needs to be scaled by the appropriate centrifuge scaling. For example, PIV generally is a very accurate instrument with resolution that can go down to 30μm at model scale, however at prototype this becomes $30\mu m \times 40g = 1.2mm$ which is worse than standard rulers. This effect is an important argument for the need to consider larger error bands for centrifuge data compared with field data, it being compounded by instrument specific issues such as the fact that calibration of bending moment gauges, especially close to the ends of instrumented plates is difficult owing to end conditions and soil pressures being notoriously difficult to measure accurately due to arching around gauges.

Since absolute errors have units which differ for each instrument type, to simplify data input, *multifit* allows specifying the absolute error as a percentage of the maximum reading to better align the format of the absolute and relative error components and to keep calculations unitless. As an example, the PIV calculation mentioned in the paragraph above shows we need to consider an absolute error of $\approx 1.2mm$ prototype, the maximum measured deflection was 12.6mm (Fig. 8a) and so we can express the absolute error as being $\approx 10\%$ of the maximum deflection measured. The *multifit* results shown in Fig. 8 were obtained considering a 10% absolute and 5% relative error on PIV data, a 25% absolute and 10% relative error on strain gauge data, a 10% absolute error on prop force as well as a 20% absolute and 40% relative error on Tekscan data. The large relative error used for Tekscan was due to the difficulties arising in calibrating the sheets in a centrifuge setting (Chan et al., 2019).

The fits shown in Fig. 8 agree well with geotechnical experience. Near-zero displacement is predicted at the base of the wall, consistent with the zero shear and net pressure predictions at the base. A pressure bulb on the retained side, behind the prop, can also be observed from the net

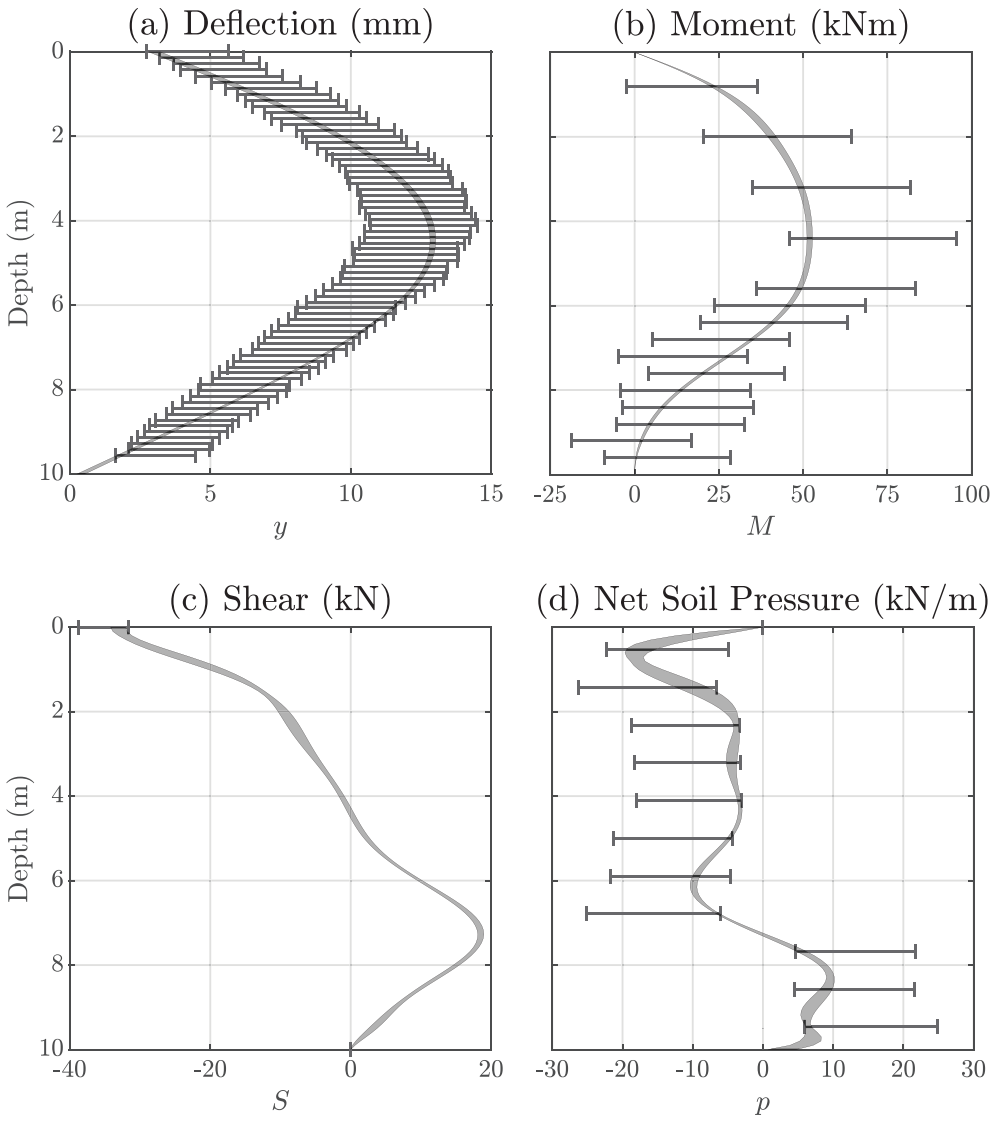

Fig. 8. Fitting noisy centrifuge data with *multifit*.

pressure consistent with the Tekscan results. Overall *multifit* produced fits consistent with both the expected wall behaviour and with all of the data available, despite errors being present in the input data.

3.3. $p-y$ analysis of data from tsunami coastal defences in Japan

Multifit is applicable not only to retaining walls but also to the analysis of laterally loaded piles since these structures also obey Eq. (1). As such, the data from a static lateral load test on a steel monopile was interpreted using *multifit*. The 15 m long, 1 m diameter pile, of the type used in tsunami walls in Japan (Dobrisan et al., 2021), was subjected to significant static lateral force by a hydraulic jack in an attempt to simulate peak tsunami wave loading. Inclinometers measured the pile rotation and strain gauges the pile curvature. Furthermore, a load cell recorded the force applied by the hydraulic jack and a displacement transducer measured the pile movement at the ground surface. A general schematic of the test setup and the instrumentation is shown in Fig. 9. Since no information was available regarding the accuracy of the measurement devices used, the recorded data was considered to have a 5% absolute and 5% relative error.

The *multifit* analysis results are presented in Fig. 10. These are plotted for the instance the loading on the pile through the hydraulic jack was 1.339MN. When laterally pushing a pile with a significant embedment we would expect the pile to rotate about a fixed point below the ground surface and, remarkably, *multifit* shows a consistent prediction of a rotation point. As highlighted in Fig. 10a and Fig. 10e, the region of predicted zero pile deflection overlaps the zero net earth pressure confidence band at around 6 m depth, indicating pile rotation around this point. Additionally, *multifit*'s prediction of small base shear at the end of the pile (Fig. 10d) is consistent with common assumptions about hollow tubular piles.

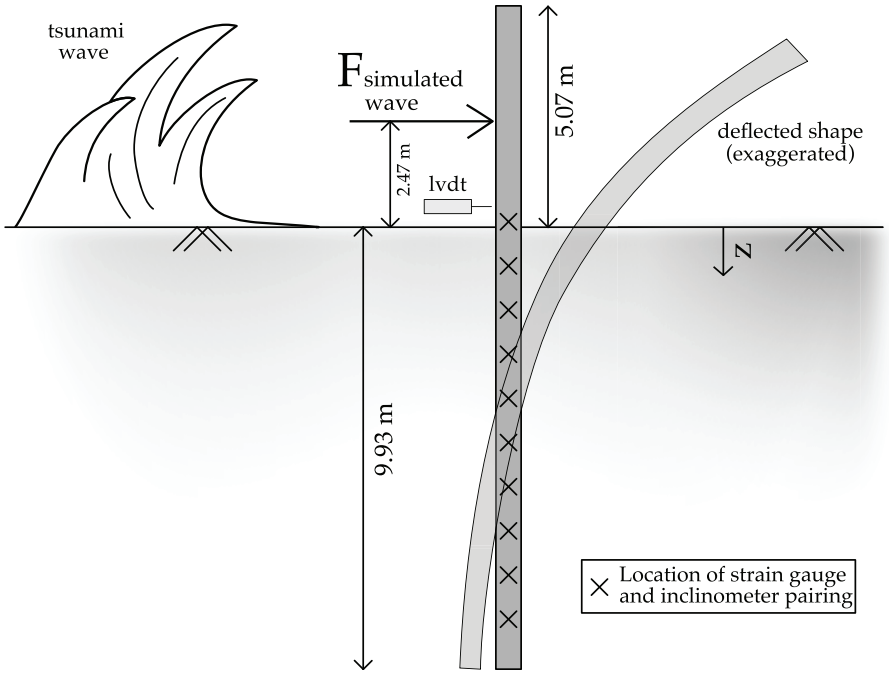

Fig. 9. Lateral loading of a steel pile with a static horizontal force simulating a tsunami scenario; adapted from Dobrisan et al. (2021).

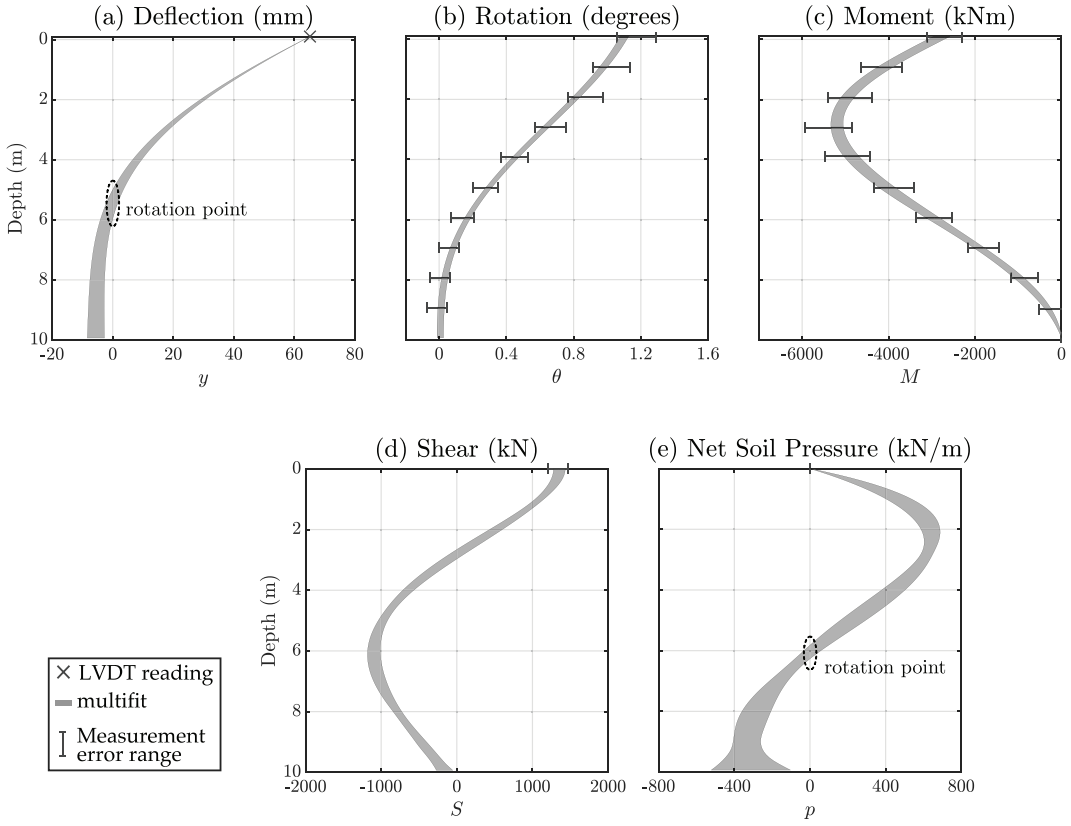

Fig. 10. Multifit analysis results for 1.339MN of horizontal loading through hydraulic jack.

Using *multifit*, predicted distributions of net soil pressure and pile displacement can be found at each depth for each loading stage during the experiment allowing for $p-y$ plots to be generated. The confidence intervals for p and y may be used to gain a measure of uncertainty on each data point on the $p-y$ plot. The *multifit* $p-y$ results at 1 m, 3 m, 8 m depth are shown in Fig. 11 and compared with design curves from Reese et al. (1974) and API

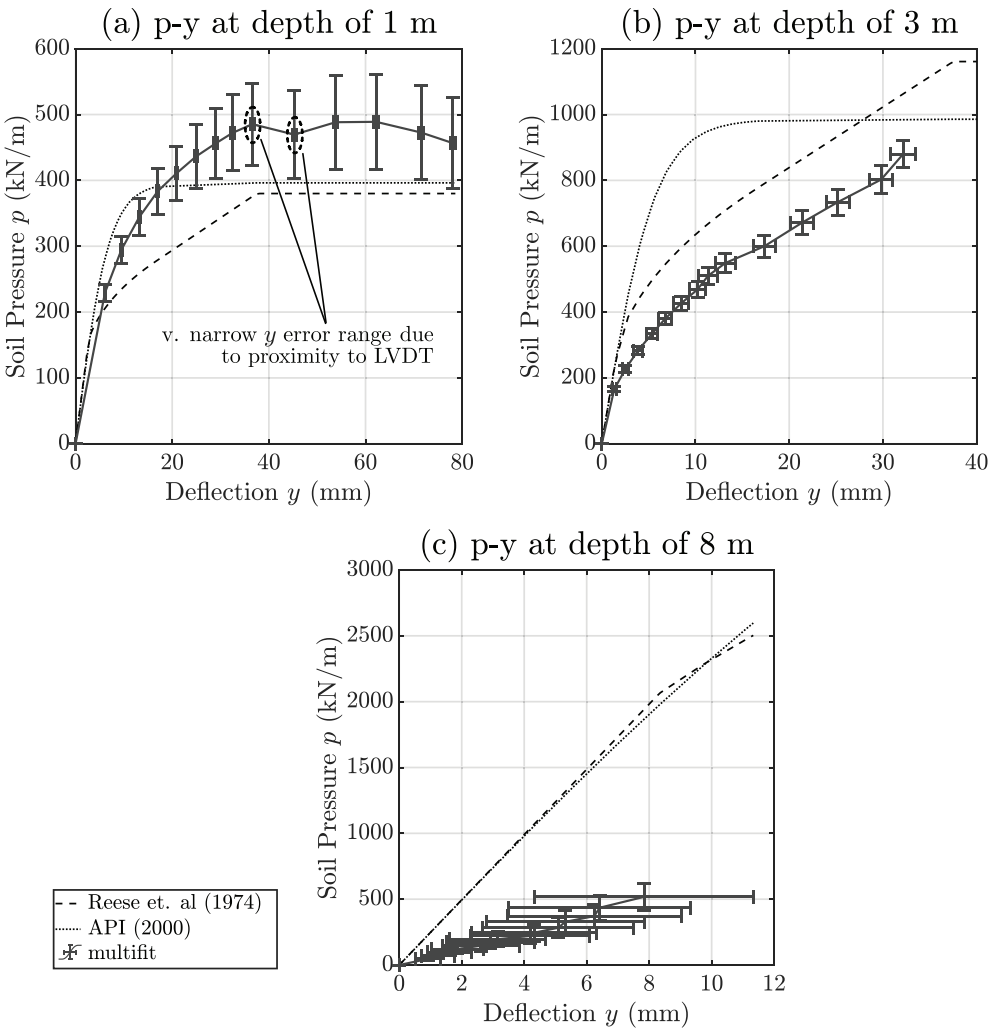

Fig. 11. $p-y$ results.

(2000). Fig. 11a evinces that, at shallow depths, there is good agreement between the experimental data analysed using *multifit* and the $p-y$ relationships proposed by Reese et al. (1974) and API (2000). However, Fig. 11b and Fig. 11c show a softer soil response than the design guidelines suggest, implying that soil stiffness may not increase with depth at the same pace as predicted by formulae commonly used in pile design.

It has so far been shown that *multifit* is a powerful technique for analysing experimental data from centrifuge tests as well as full-scale experiments, with applicability to retaining wall structures and monopiles. However, because generally in experiments the true distribution of parameters such as earth pressure, bending moment etc. is unknown, the assessment of the quality of the fits is limited to qualitative checks against known geotechnical behaviour (such as the existence of a rotation point in the monopile example above). To obtain quantitative measurements of fit quality, *multifit* needs to be used in a scenario in which the true retaining wall behaviour is known beforehand. The easiest way to achieve this goal is to construct a theoretical retaining wall problem with prescribed earth pressure distributions.

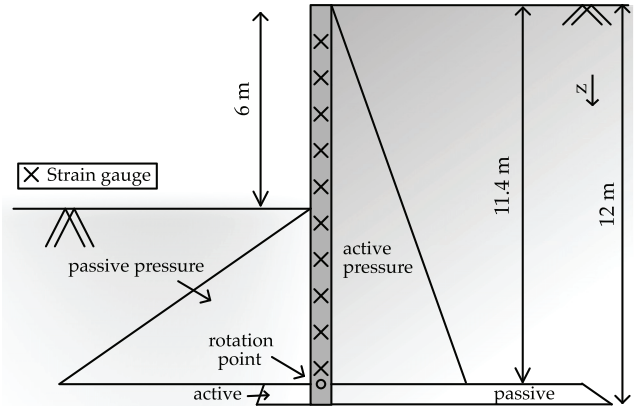

Fig. 12. ULS Retaining wall problem with active and passive pressures dictated by Coulomb (1776) and Rankine (1857) theories.

4. Theoretical validation

4.1. Ultimate Limit State (ULS) design scenario with net pressure discontinuities

For this theoretical experiment, we consider the setup shown in Fig. 12 of a 12 m sheet pile retaining wall supporting a 6 m deep excavation. The soil considered is a sand with unit weight γ of 20kN/m^3 and friction angle Φ of 30°. Ten equidistant bending moment readings are simulated based on the theoretical solution with 5% absolute and 5% relative errors being randomly generated to model experimental inaccuracies.

The choice of polynomial order is an important parameter in *multifit* analysis as it involves a trade-off between possible solution geometries and computational time. To assess this trade-off, the earth pressure profile was set to include sharp discontinuities by matching Coulomb (1776) and Rankine (1857) theories at ultimate limit state (ULS). Since *multifit* fits the available data with high order polynomials, these discontinuties can never be exactly fitted, but their approximation should improve with increasing fit order.

As shown in Fig. 13, *multifit* using 10th order polynomials does a good job in predicting the ULS wall behaviour even with sharp changes in the net pressure distribution at the excavation level and point of rotation. Although the rapid change in net pressure at the rotation point is somewhat outside the confidence bands, the fitted pressure profile captures the important aspects of the soil-structure interaction with good accuracy. The excavated depth of 6 m and the passive pressure generation on the excavated side are well predicted. Moreover the wall's rotation point, corresponding to a zero net pressure point at depth, is estimated by *multifit* as being in the range 11.0 m–11.3 m, very close to the exact solution of 11.4 m.

4.2. Fit accuracy vs computational time

The results shown in Fig. 13 were obtained using 10th order polynomials fitted to the data set. The order refers to the polynomials fitting the parameter highest in the differentiation chain, in this case moment. The net pressure fits are consequently 8th order polynomials. Changing the order modifies the predictions and the associated confidence bands. By utilising the known ULS behaviour for the retaining wall in Fig. 12 we can investigate the errors in the *multifit* results as a function of the polynomial order of the highest parameter in the differentiation chain (i.e. moment).

Each individual *multifit* analysis gave confidence intervals for moment, shear and pressure, the centres of which were compared to the theoretical solution. This difference was considered to be representative of the error in the analysis and its RMS value across the depth of the wall divided by the absolute maximum theoretical value was used to obtain dimensionless relative errors for each physical quantity. Fig. 14a shows the change in RMS error as a function of the polynomial order of the moment fit (as discussed in the previous paragraph).

It can be seen that initially, with increasing polynomial order, the errors decrease significantly, stabilising around the 8th order fit. Irrespective of polynomial order, the moment error is smallest, followed by the shear error with the pressure displaying the largest deviation from the true solution. Intuitively this makes sense, since *multifit* was provided moment data and each differentiation step amplifies the fitting errors of the previous step. A compounding factor in the increase in error for net pressure is the disproportionate influence of the sudden change from large positive to similarly large negative values at the rotation point. A relatively small error in predicting this localised behaviour disproportionately affects the RMS due to taking the square of localised large values. However, it is encouraging to observe that, even in these circumstances, the RMS error on pressure can be as low as 11%.

The excavation depth and the position of the wall's rotation point are significant geotechnical parameters and the accuracy in predicting these properties was also evaluated. The two centres of the confidence band's intersections with the zero net pressure axis, corresponding to the predictions of excavated depth and rotation point respectively, were compared and normalised against the theoretical values. For the case the theoretical points were within the confidence bands the error was considered to be zero. The resulting plot is shown in Fig. 14b. For low polynomial orders the second change in net pressure sign, indicative of rotation point, did not occur (as shown in Fig. 15a). Thus prediction of rotation point are only available for orders larger than 7. From Fig. 14b it can be seen that both the excavation depth and the rotation point location are predicted with very little error for the higher polynomial orders.

An important advantage of *multifit*'s approach of finding all polynomials that satisfy the problem is that it is significantly less sensitive to the oscillatory behaviour of high order polynomials than standard polynomial fitting. Generally it might be expected that once the polynomial order is high enough to fit the data set well, further increases in the polynomial order will not bring about significant improvements to the fit or changes in predictions. A further illustration of this point is the comparison between the net pressure distributions predicted by 6th, 10th and 12th order *multifit* as shown in Fig. 15.

The 6th order prediction includes a number of significant geotechnical inconsistencies, such as lacking the ability to predict the existence of a net pressure change at the rotation point. The 10th order fit quantifies accurately both the excavation depth and the position of the rotation point. With the 12th order fit we see similar predictions of the above mentioned properties but also the ability to model the rapid change in gradient past the rotation point. This

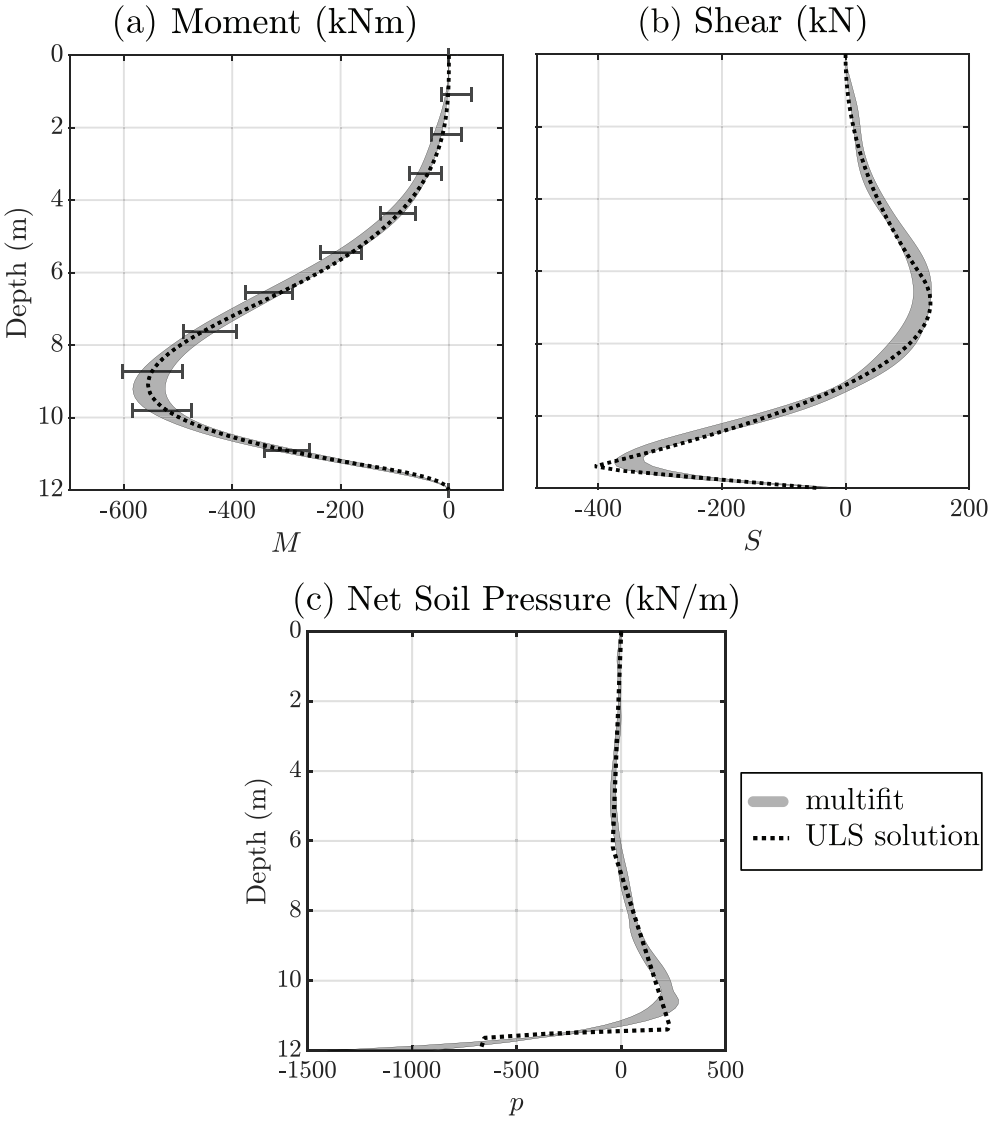

Fig. 13. Comparison between *multifit* prediction and ULS solution.

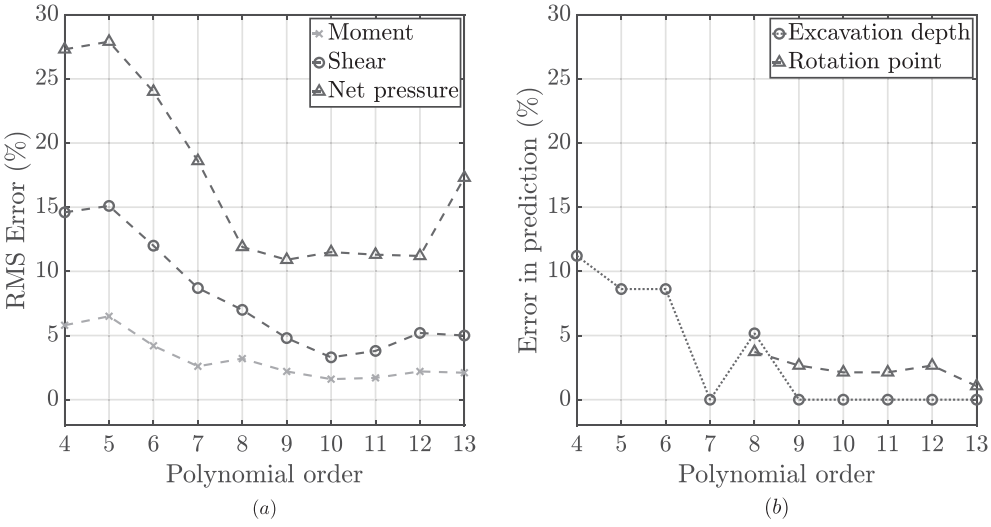

Fig. 14. Relative errors in prediction against polynomial order.

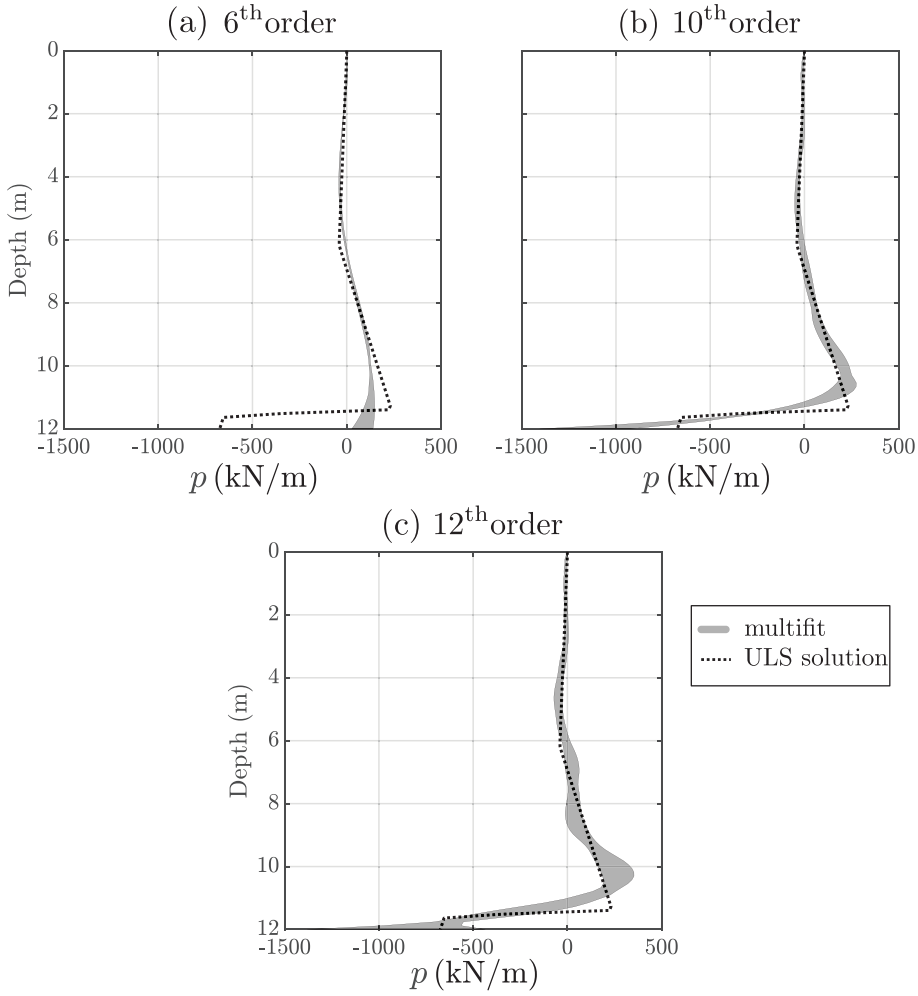

Fig. 15. Comparison of net pressure predictions with increasing polynomial order.

result is, however, not useful since the confidence bands are very large due to no data being available at the retaining wall base. Hence, from a geotechnical perspective, there is little benefit in utilising the 12th order fit.

While higher order fits are generally better, this comes at the expense of computational time. Because *multifit* returns a family of polynomials that represent all possible solutions of a given polynomial order that fit the data set, increasing the polynomial order is equivalent to adding an extra dimension to the problem so the complexity increases exponentially. Specifying exact known constraints such as zero moments at the free ends of the wall can partially mitigate this issue, as each such constraint reduces the number of free variables by one.

The run times for the *multifit* analyses presented in Fig. 14 are shown in Table 1. The number of free variables is written alongside the polynomial order since it is the property most strongly correlated with the run time. Most analysis was carried on a standard personal computer (PC). Due to the exponential increase of run time with the number of free variables, the high order runs were computed using the Peta 4 supercomputer at Cambridge University. Finding the fit polynomials is a highly parallel task so the run time significantly reduces with the number of CPU cores available for analysis.

It can be seen from Table 1 that even higher order analyses can be calculated on personal computers with modest runtimes. Moreover multi-core machines can be used to decrease run time almost linearly with the number of CPUs available.

Table 1
Multifit run times.

Polynomial order (free variables)	Run time on PC	Run time on Peta 4
4(2)	2 s	
5(2)	2 s	
6(3)	3 s	
7(4)	4 s	
8(4)	4 s	
9(5)	9 s	
10(6)	4 min	
11(7)	35 min	
12(8)	78h17 min	4 h
13(9)		57 h38 min

5. Conclusions

This paper introduces a novel routine for the common problem of interpreting retaining wall data to derive information on soil-structure interaction. *Multifit* presents advantages over conventional methods including the ability to pull together imperfect data from a multitude of instruments (strain gauges, inclinometers, LVDTs, Tekscan, PIV etc.) into a cohesive prediction. Moreover, the method outputs a representative sample of all polynomials of a given order that satisfy the inputs allowing a measure of uncertainty to be quantified.

Analysis of field and centrifuge data demonstrated *multifit* outperforming existing fitting solutions in capacity to discern the underlying continuous profile in noisy sparse data and in the depth of differentiation to which meaningful information could still be retrieved. The capability of the technique was also investigated by analysing a challenging theoretical problem in which *multifit* showed significant increases in accuracy at higher orders for both the directly measured property (moment) and its derivatives (shear and net soil pressure). This is a marked improvement over conventional techniques which at higher orders fit data increasingly well at the expense of spurious oscillations that end up dominating the behaviour once the property is differentiated.

Overall, the results paint an encouraging perspective for the benefit this new method may bring to data analysis in the context of retaining wall and lateral pile testing.

Using *multifit*

The *multifit* method has been implemented as a MATLAB function and can be freely downloaded from `github.com/andrei-dobrisan/multifit`. The link also features relevant documentation and examples to show how the code can be used and integrated into geotechnical research.

Acknowledgements

The authors are grateful to EPSRC for support in the form of a Doctoral Training Award to A.D, Grant No. EP/M508007/1. The support of Giken Ltd. in providing the data from the pile lateral loading experiment is gratefully acknowledged.

This work was performed using resources provided by the Cambridge Service for Data Driven Discovery (CSD3) operated by the University of Cambridge Research Computing Service (www.csd3.cam.ac.uk), provided by Dell EMC and Intel using Tier-2 funding from the Engineering and Physical Sciences Research Council (capital grant EP/P020259/1), and DiRAC funding from the Science and Technology Facilities Council (www.dirac.ac.uk).

References

API, 2000. Recommended Practice for Planning, Designing and Constructing Fixed Offshore Platforms-Working Stress Design. Technical Report 2A-WSD.

Burali d'Arezzo, F., Haigh, S.K., Talesnick, M., Ishihara, Y., 2015. Measuring horizontal stresses during jacked pile installation. ICE Proc.: Geotech. Eng. 168, 306–318. https://doi.org/10.1680/geng.14.00069.

Chan, D., Madabhushi, G., Deng, C., Haigh, S., 2019. Calibration of tactile pressure sensing mats for static geotechnical centrifuge applications. Technical Report 349. University of Cambridge.

Coulomb, C.A., 1776. Essai sur une application des règles des maximas et minimas à quelques problèmes de statique relatifs à l'architecture. Mém. acad. roy. pres. divers savanta 7, 343–382.

Dantzig, G.B., 1951. Maximization of a linear function of variables subject to linear inequalities. Activity Analysis of Production and Allocation. Wiley & Chapman-Hall, New York, pp. 339–347.

Deng, C., 2020. Sand Deformation Mechanisms and Earth Pressures Mobilised with Retaining Wall Movements. PhD. University of Cambridge. Cambridge.

Deng, C., Haigh, S.K., Ma, X., Xu, J., 2021. A design method for flexible retaining walls in clay. Géotechnique 71, 178–187. https://doi.org/10.1680/jgeot.19.P.095.

Diaconis, P., Freedman, D., 1986. On the consistency of Bayes estimates. Ann. Stat. 14, 1–26.

Dobrisan, A., Haigh, S.K., Ishihara, Y., 2021. Experimental evaluation of the lateral capacity of large jacked-in piles and comparison to existing design standards. In: Proceedings of the Second International Conference on Press-in Engineering 2021, Kochi, Japan, CRC Press. pp. 218–223.

Haiderali, A.E., Madabhushi, G., 2016. Evaluation of curve fitting techniques in deriving p–y curves for laterally loaded piles. Geotech. Geol. Eng. 34, 1453–1473. https://doi.org/10.1007/s10706-016-0054-2.

Li, A., Lehane, B., 2010. Embedded cantilever retaining walls in sand. Géotechnique 60, 813–823. https://doi.org/10.1680/geot.8.P.147.

Paikowsky, S., Hajduk, E., 1997. Calibration and use of grid-based tactile pressure sensors in granular material. Geotech. Test. J. 20, 218–241. https://doi.org/10.1520/GTJ10741J.

Rankine, W.J.M., 1857. On the stability of loose earth. Philosophical Trans. Royal Soc. 147, 9–27.

Reese, L.C., Cox, W.R., Koop, F.D., 1974. Analysis of laterally loaded piles in sand. Sixth Annual Offshore Technological Conference, Houston, Texas, pp. 473–483.

Talesnick, M., 2005. Measuring soil contact pressure on a solid boundary and quantifying soil arching. Geotech. Test. J. 28, 171–179. https://doi.org/10.1520/GTJ12484.

Timoshenko, S., 1953. History of Strength of Materials. McGraw-Hill, New York.

Weierstrass, K., 1885. Über die analytische Darstellbarkeit sogenannter willkürlicher Functionen einer reellen Veränderlichen. Sitzungsberichte der Königlich Preußischen Akademie der Wissenschaften zu Berlin 2, 633–639.

Weiler, W.A., Kulhawy, F.H., 1982. Factors affecting stress cell measurements in soil. J. Geotech. Eng. Divis 108, 1529–1548.

White, D.J., Take, W., Bolton, M.D., 2003. Soil deformation measurement using particle image velocimetry (PIV) and photogrammetry. Geotechnique 53, 619–631.